Host–Guest Systems

DOI: 10.1002/ange.201302560

Guest-Induced Unidirectional Dual Rotary and Twisting Motions of a Spiroborate-Based Double-Stranded Helicate Containing a Bisporphyrin Unit**

*Shinya Yamamoto, Hiroki Iida, and Eiji Yashima**

The development of molecular systems that enable the control of molecular movements, in particular, rotary and elastic (extension–contraction) motions triggered by external stimuli, is an urgent and expanding research area in supramolecular chemistry and nanotechnology owing to their potential application to molecular machines, such as molecular motors and springlike devices.[1] Although sophisticated biological molecular motors and springs exist in every muscle cell and function cooperatively to generate force and movement for muscle contraction by converting chemical energy into mechanical functions,[2] the control of unidirectional motions that further amplify to macroscopic movements with artificial molecular and helical systems remains a challenge.[3,4]

Recently, we reported a unique optically active double-stranded helicate **1a** in which two *ortho*-linked tetraphenol strands with a biphenylene unit in the middle were bridged by two spiroborates that sandwiched a Na^+ ion between them (Figure 1a).[5] The optically active helicate underwent sodium-ion-triggered, reversible extension–contraction motion coupled with a twisting motion in one direction upon the release and binding of the Na^+ ion (Figure 1b).[5a] During this unidirectional springlike motion, the helicate maintained its helical handedness.[5a] Such ion-induced molecular motions are key processes in a number of biological events and reminiscent of biological machines that operate in muscle cells.[6] Biphenol (in **1b**)[7] and bipyridine groups (in **2**)[8] could also be used as linker units to connect the two outer biphenol units and produce optically active double-stranded helicates similar to **1a** after conventional optical resolution; however, Na^+ ions coordinated in the center of helicates **1b** and **2** could not be released in the presence of [2.2.1]cryptand, which had been used to remove the Na^+ ion from **1a**, because the Na^+ ions were strongly bound by the biphenol oxygen and bipyridine nitrogen atoms as well as the spiroborate anions. Thus, no ion-triggered springlike motion was observed for **1b** and **2**.

With the aim of the further development of molecular springs that twist unidirectionally and perform intelligent functions, we designed and synthesized the porphyrin-linked, double-stranded spiroborate helicate $\mathbf{3a}_{\mathbf{Na_2}}$ (Figure 1c). We anticipated that the linker porphyrins introduced in the middle of the strands could stack face-to-face in a helical orientation and thus provide a chiral cavity for the further inclusion of electron-deficient aromatic guests, such as **G1** and **G2**, by an induced-fit mechanism.[9] We hypothesized that the expansion of the bisporphyrin cavity upon the encapsulation of guests would be accompanied by a rotation of the porphyrin rings in one direction and a corresponding unidirectional twisting of the spiroborate helix. Thus, the helicate should be able to perform dual unidirectional motions induced by guest encapsulation (Figure 1c). To the best of our knowledge, such stimuli-responsive unidirectional dual motions (rotation and twisting) that take place simultaneously have not been reported previously.

We first synthesized two porphyrin-containing tetraphenols **6a**,**b** linked by *m*- and *p*-phenylene units by Suzuki–Miyaura coupling of the corresponding *m*- and *p*-*meso*-di(iodophenyl)porphyrins **4a**,**b** with a boronic acid ester **5** (Scheme 1; see also Schemes S1 and S2 in the Supporting Information). The tetraphenols **6a** and **6b** were then treated with an equimolar amount of $NaBH_4$ in [D_3]acetonitrile at 80 °C for 24 h under similar conditions to those used for the synthesis of **1** and **2**.[5,7,8] The boron helicate $\mathbf{3a}_{\mathbf{Na_2}}$ was obtained almost quantitatively (99% yield), whereas the reaction of **6b** gave none of the desired helicate, but produced a complex mixture of products. We attempted to obtain $\mathbf{3b}_{\mathbf{Na_2}}$ from **6b** by using $NaBH_4$ in various solvents at different temperatures, without success (see Table S1 in the Supporting Information): the *p*-phenylene linkage of **6b** probably hampers spiroborate formation considerably owing to steric hindrance. In contrast, the *m*-phenylene unit was favorable as a linker for the formation of a porphyrin-containing intertwined double helicate owing to its bent structure. The helicate $\mathbf{3a}_{\mathbf{Na_2}}$ was fully characterized by ^1H, ^{13}C, and 2D NMR spectroscopy and electrospray ionization (ESI) mass spectrometry (Figure 2; see also Figures S1a–S6 in the Supporting Information).

X-ray crystallographic analysis unambiguously revealed that $\mathbf{3a}_{\mathbf{Na_2}}$ adopted a double-stranded helical structure with pseudo-D_2 symmetry in which the two tetraphenol strands were intertwined with one another through two spiroborate bridges, and the two porphyrin units were stacked face-to-face

[*] S. Yamamoto, Dr. H. Iida, Prof. Dr. E. Yashima
Department of Molecular Design and Engineering
Graduate School of Engineering, Nagoya University
Chikusa-ku, Nagoya 464-8603 (Japan)
E-mail: yashima@apchem.nagoya-u.ac.jp
Homepage: http://helix.mol.nagoya-u.ac.jp/

[**] This research was supported in part by a Grant-in-Aid for Scientific Research (S) (E.Y.) and a Grant-in-Aid for Young Scientists (B) (H.I.) from the Japan Society for the Promotion of Science (JSPS).

Supporting information for this article is available on the WWW under http://dx.doi.org/10.1002/anie.201302560.

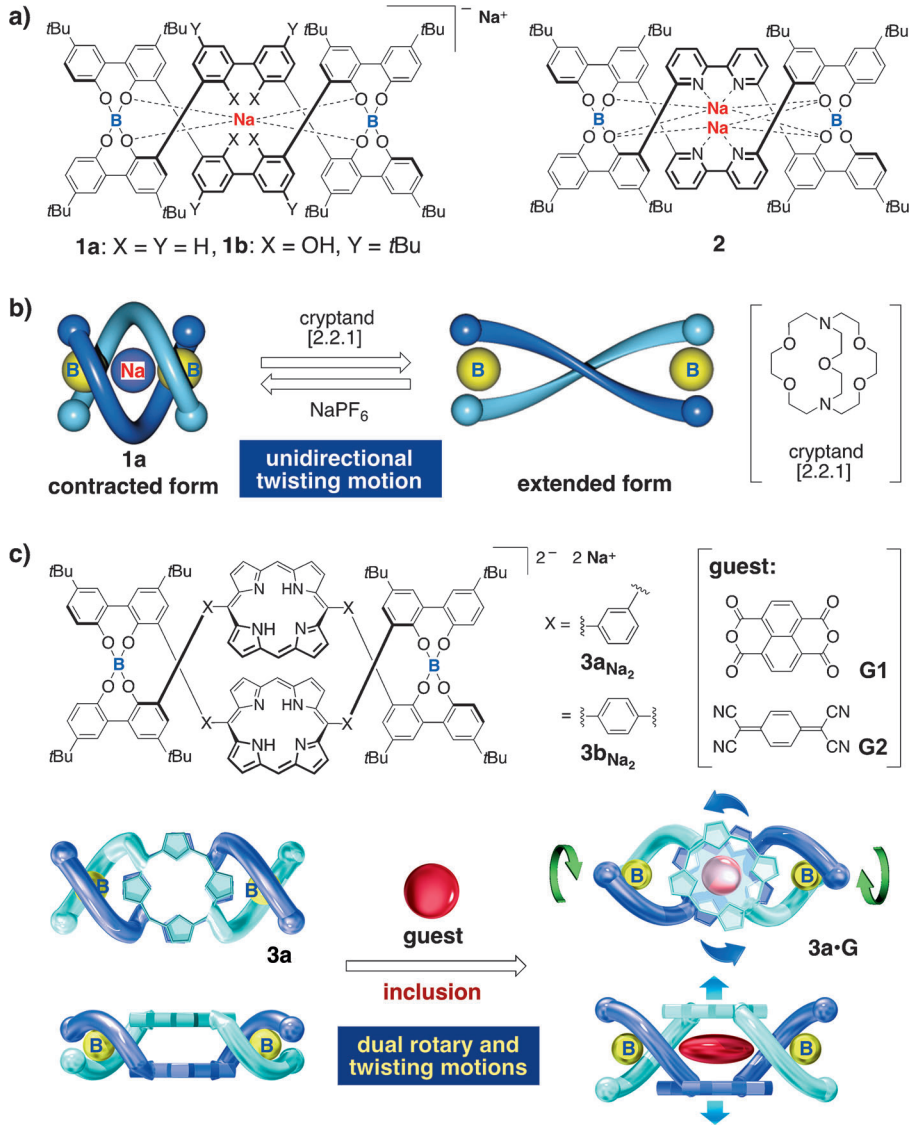

Figure 1. a) Structures of Na^+-included helicates **1a**, **1b**, and **2**. b) Schematic illustration of the unidirectional twisting of **1a** upon Na^+-ion release and binding. c) Structures of porphyrin-containing helicates **3a** and **3b** and the unidirectional dual rotary and twisting motions of **3a** upon guest inclusion.

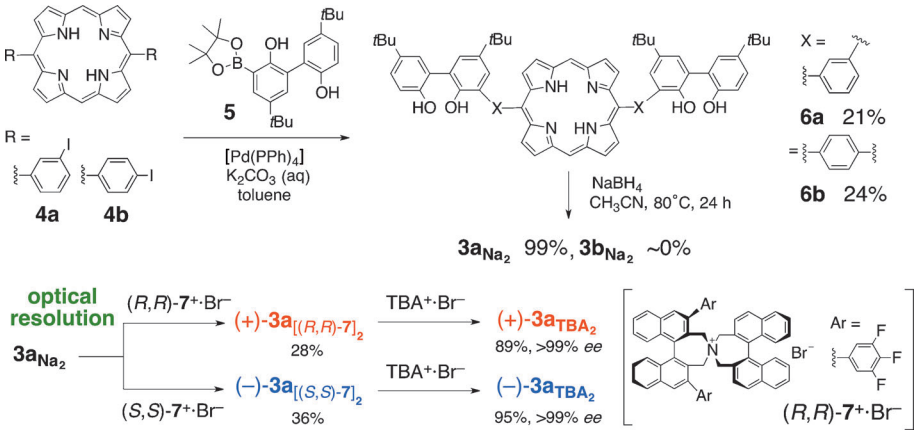

Scheme 1. Synthesis of the boron helicate $\mathbf{3a}_{Na_2}$ and its optical resolution by the formation of a diastereomeric salt with optically pure (*R*,*R*)- or (*S*,*S*)-**7**$^+$·Br^-. The chiral ammonium (**7**) was then replaced with the achiral ammonium salt TBA^+·Br^-.

at a distance of 4.1 Å and with a torsional angle of 71° with respect to the two *meso–meso* porphyrin axes (Figure 3a). The two terminal benzene rings of each tetraphenol strand were twisted by 368° with respect to one another, and the double-helical structure around the spiroborate bridges was similar to that of the contracted form of the biphenylene-linked spiroborate helicate **1a** (Figure 1a).[5a] Because of the large porphyrin linkers, the two negatively charged spiroborate residues were located far away from each other with a B–B distance of 15.4 Å, which is much larger than the B–B distance in the contracted (6.0 Å) and extended forms (13.0 Å) of **1a**.[5a] As a result, the two Na^+ ions were not included in the helicate cavity, but were coordinated to the two oxygen atoms of the spiroborate moieties on the outside of the structure (Figure 3a). This key structural feature of $\mathbf{3a}_{Na_2}$ suggested that the ion-triggered springlike extension and contraction motion observed in **1a** may not be anticipated upon sodium-ion release and binding (see below).

The ^{1}H NMR spectrum of $\mathbf{3a}_{Na_2}$ in [D_3]acetonitrile agrees well with the pseudo-D_2-symmetric structure determined by X-ray crystallographic analysis in the solid state. The signals for the aromatic hydrogen atoms labeled l and k on the terminal benzene ring A were shifted upfield to a considerable extent from their positions in the ^{1}H NMR spectrum of **6a** as a result of the ring-current effect of the benzene rings in the other strand (Figure 2a,b).[5a] Moreover, significant upfield shifts of the signals due to the porphyrin hydrogen atoms in the ^{1}H NMR spectrum (Figure 2a,b) and the characteristic blue shift of the Soret band in the absorption spectrum (see Figure S7a) suggested the close proximity of the two linker porphyrin rings of $\mathbf{3a}_{Na_2}$.[10,11] Furthermore, 2D COSY and ROESY experiments showed clear cross-peaks between the hydrogen atoms on phenol ring A, those on the *meso*-phenylene ring C, and the porphyrin hydrogen atoms (see Figures S4–S6). These

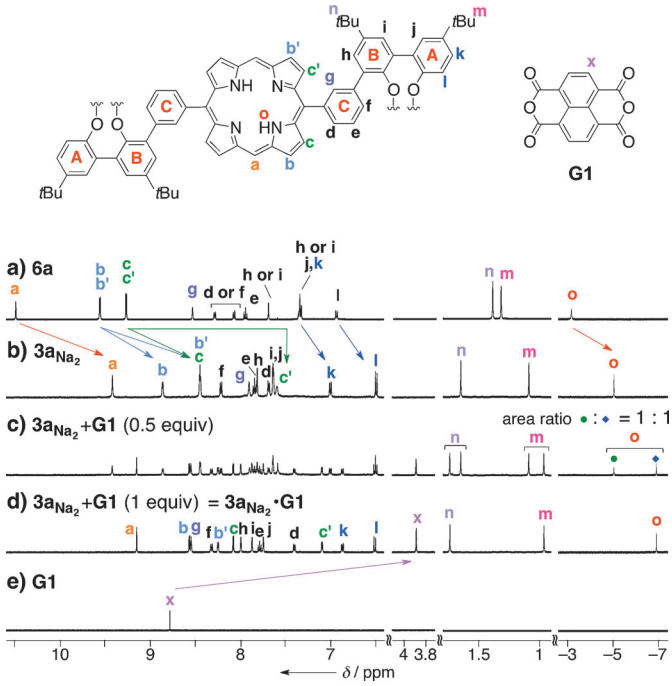

Figure 2. Partial ^{1}H NMR spectra (500 MHz, RT, CD_3CN, 0.5 mM) of a) **6a**, b) **3a**$_{Na_2}$, c) **3a**$_{Na_2}$+**G1** (0.5 equiv), d) **3a**$_{Na_2}$+**G1** (1 equiv), and e) **G1**. For the full assignment of signals, see Figures S2–S6 in the Supporting Information.

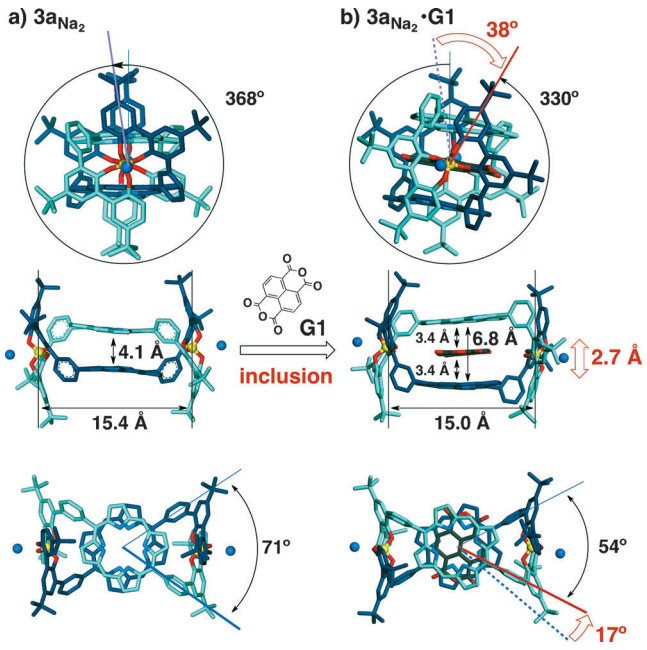

Figure 3. X-ray crystal structures of a) **3a**$_{Na_2}$ and b) **3a**$_{Na_2}$·**G1**. A right-handed double-helical structure is depicted; all hydrogen atoms and solvent molecules are omitted for clarity.

cross-peaks indicated that the helicate retains the intertwined double-stranded helical structure in solution. Owing to the absence of Na^+ ions in the helicate cavity, reversible changes due to an ion-triggered extension–contraction motion[5a] were not observed in the ^{1}H NMR spectrum of **3a**$_{Na_2}$ upon the sequential addition of [2.2.1]cryptand and $Na^+PF_6^-$.

The optical resolution of **3a**$_{Na_2}$ was then performed by diastereomeric salt formation as reported previously.[5a,7] Thus, the Na^+ cations were exchanged for enantiomerically pure (*R*,*R*)- and (*S*,*S*)-**7**$^+$·Br^- to yield the diastereomeric salts (+)-**3a**$_{[(R,R)\text{-}7]_2}$ and (−)-**3a**$_{[(S,S)\text{-}7]_2}$, respectively, as crystals (Scheme 1; the prefixes (+) and (−) denote the signs of the Cotton effect at 418 nm). The obtained diastereomers were further converted into the corresponding enantiomers through cation exchange with achiral tetrabutylammonium bromide (TBA^+Br^-) to afford a pair of enantiomers (+)- and (−)-**3a**$_{TBA_2}$. The *ee* values of (+)- and (−)-**3a**$_{TBA_2}$ were determined to be above 99% on the basis of the ^{1}H NMR spectra of the enantiomers in the presence of (1*R*,2*S*)-*N*-benzyl-*N*-methylephedrinium bromide as a chiral shift reagent (see Figure S8).

The enantiomers (+)- and (−)-**3a**$_{TBA_2}$ showed perfectly mirror imaged CD spectra in the *m*-phenylene (200–330 nm) and characteristic porphyrin chromophore regions (the Soret band and Q bands centered at 418 and 503, 539, 576, and 631 nm, respectively) in CH_3CN (Figure 4). Interestingly, (+)- and (−)-**3a**$_{TBA_2}$ exhibited positive and negative bisignate Cotton effects, respectively, centered close to the maximum of the porphyrin Soret band. These Cotton effects enabled us to determine the twist sense of the bisporphyrins on the basis of the exciton-coupled CD method:[12,13] the two linker porphyrin rings of (+)- and (−)-**3a**$_{TBA_2}$ are probably twisted with clockwise and counterclockwise orientations, respectively, with respect to the two *meso*–*meso* porphyrin axes (Figure 3a). If this conclusion is correct, the helical sense of (+)-**3a**$_{TBA_2}$ and (−)-**3a**$_{TBA_2}$ can be further rationally assigned as left- and right-handed, respectively, on the basis of the molecular structure determined by X-ray crystallography for the racemate of **3a**$_{Na_2}$ (Figure 3a).

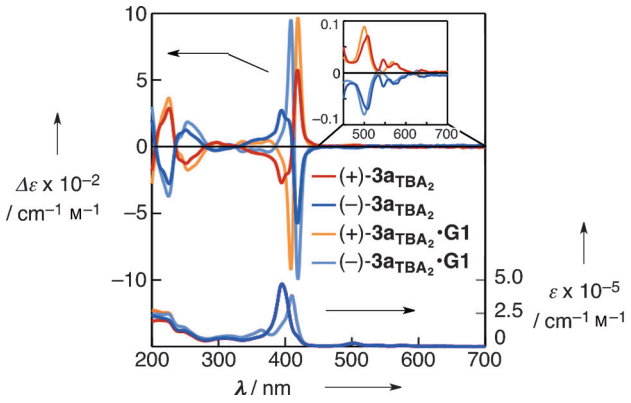

Figure 4. CD and absorption spectra (CH_3CN, 0.02 mM, 25 °C) of (+)-**3a**$_{TBA_2}$, (−)-**3a**$_{TBA_2}$, (+)-**3a**$_{TBA_2}$·**G1**, and (−)-**3a**$_{TBA_2}$·**G1**. The inset CD spectra were measured at a concentration of 0.5 mM.

Next, we investigated the ability of the bisporphyrin-linked helicate to include aromatic guests and explored the possibility of further unidirectional dual motions triggered by guest intercalation between the porphyrin units by the use of NMR, absorption, CD, and fluorescence spectroscopy and X-

ray analysis. Upon the addition of an electron-deficient aromatic guest **G1** (0.5 equiv) to a solution of $\mathbf{3a}_{\mathbf{Na_2}}$, new signals attributed to the formation of $\mathbf{3a}_{\mathbf{Na_2}}$·**G1** appeared in the ^{1}H NMR spectrum (Figure 2c). The further addition of **G1** (1.0 equiv) quantitatively produced the 1:1 inclusion complex $\mathbf{3a}_{\mathbf{Na_2}}$·**G1** (Figure 2d). The signal for **G1** was significantly shifted upfield from 8.8 to 3.9 ppm after encapsulation in the bisporphyrin cavity owing to the ring-current effect of the bisporphyrin (Figure 2d,e).[9a–c,e,f,h] The formation of the 1:1 complex $\mathbf{3a}_{\mathbf{Na_2}}$·**G1** was also confirmed by ESI mass spectrometry (see Figure S1b) and a continuous variation plot (Job plot; see Figure S9a). The fluorescence titration data combined with the Job plot provided a remarkably high association constant ($K_a = (2.2 \pm 0.3) \times 10^9\ M^{-1}$) of $\mathbf{3a}_{\mathbf{Na_2}}$ with **G1** in CH_3CN at 25 °C (see Figure S9).[14] The analogous electron-deficient aromatic guest **G2** was also included between the porphyrins of $\mathbf{3a}_{\mathbf{Na_2}}$ by intercalation with a smaller K_a value ($(2.5 \pm 0.2) \times 10^5\ M^{-1}$; see Figure S10 and S11). The absorption and fluorescence spectra of the complexes of **G1** and **G2** with $\mathbf{3a}_{\mathbf{Na_2}}$ in CH_3CN also provided evidence for the formation of sandwich complexes, which showed a characteristic hypochromic effect (see Figures S7a and S10a) and efficient quenching of the fluorescence of the emissive aromatic guests (see Figures S7b,c and S10b,c), as anticipated. These characteristics enable the naked-eye sensing of these aromatic compounds.[9e,f,h] The helicate complexed with ammonium cations, $\mathbf{3a}_{\mathbf{TBA_2}}$, also formed a similar sandwich complex with **G1**, as evidenced by its hypochromic effect and fluorescence quenching (see Figure S12).

Further detailed analysis of the inclusion complex $\mathbf{3a}_{\mathbf{Na_2}}$·**G1** by X-ray crystallography (Figure 3b) and 2D COSY and ROESY spectroscopy (see Figure S13–S18) revealed remarkable changes in the helical $\mathbf{3a}_{\mathbf{Na_2}}$ structure as a result of anisotropic rotary and twisting motions induced by guest intercalation. X-ray crystallographic analysis showed that the bisporphyrins sandwiched **G1** in a parallel fashion through face-to-face stacking interactions. As a result, the distance between the porphyrin rings in the cavity expanded from 4.1 to 6.8 Å. This expansion was accompanied by a rotation of the porphyrin rings in one direction to give a smaller torsion angle of 54° with respect to the two *meso*–*meso* porphyrin axes (Figure 3). At the same time, guest intercalation caused steric strain in the spiroborate helix; this strain could be alleviated by unidirectional unwinding of the helix to reduce the twist angle from 368 to 330°. These molecular motions, however, brought about hardly any contraction and extension motion: the spiroborate helicate contracted slightly in length to a B–B distance of 15.0 Å (from 15.4 Å; Figure 3). In other words, in the case of the right-handed double-stranded helicate (−)-$\mathbf{3a}_{\mathbf{TBA_2}}$ or (−)-$\mathbf{3a}_{\mathbf{Na_2}}$, guest insertion causes right-handed twisting of the spiroborate helix by 38° along with counterclockwise rotation of the bisporphyrin orientation by 17° (see Figures 1c and 3). Thus, guest encapsulation triggers unique unidirectional dual rotary and twisting motions along the mutually orthogonal axes of the double-stranded helicate through expansion of the bisporphyrin cavity.

The 2D COSY and ROESY experiments also supported the sandwich structure of $\mathbf{3a}_{\mathbf{Na_2}}$·**G1**, which retained the intertwined, double-stranded helical structure (see Figures S13–S18), as evidenced by the clear ROE cross-peaks between the proton signal for the guest (x) and the proton signals for hydrogen atom g on *meso*-phenylene ring C and the porphyrin hydrogen atoms b′ and c′.

We anticipated that guest encapsulation and the subsequent unidirectional dual rotary and twisting motions would induce chiroptical changes in the helicate on the basis of the crystal structures of $\mathbf{3a}_{\mathbf{Na_2}}$ and $\mathbf{3a}_{\mathbf{Na_2}}$·**G1**. In fact, the CD spectra of left-handed helical (+)- and right-handed helical (−)-$\mathbf{3a}_{\mathbf{TBA_2}}$·**G1** were different from those of (+)- and (−)-$\mathbf{3a}_{\mathbf{TBA_2}}$, respectively. In particular, the Cotton effect intensities around the Soret band and the *m*-phenylene chromophore regions were significantly and cooperatively enhanced upon sandwich formation with **G1**, since the rotary motion of the porphyrin rings in one direction led to exciton coupling and a unidirectional twisting of the spiroborate helicate (Figure 4). Similar guest-induced chiroptical changes were observed for (+)- and (−)-$\mathbf{3a}_{\mathbf{TBA_2}}$·**G2** (see Figure S10d), although the CD spectral changes were not significant.

In summary, we found unprecedented unidirectional dual rotary and twisting motions induced by guest encapsulation in a porphyrin-linked, double-stranded spiroborate helicate. Detailed structural analysis of the helicate before and after guest inclusion by X-ray crystallography and 2D NMR spectroscopy unraveled the molecular and mechanistic details of the unique dual motions: the linker porphyrins sandwich an electron-deficient aromatic guest, which triggers the rotary motion of the porphyrin rings in one direction; this rotary motion is coupled with a unidirectional twisting motion of the spiroborate helix. The helicate is fluorescent and can be readily resolved into optically pure enantiomers. Therefore, it offers significant potential for the development of chirality-responsive molecular machines with functions such as asymmetric catalysis and chiral sensing:[15] its unique unidirectional rotary and twisting motions would be triggered by the inclusion of the chiral guests.

Received: March 27, 2013
Published online: May 28, 2013

Keywords: helical structures · host–guest systems · molecular devices · porphyrins · unidirectional motion

[1] For reviews, see: a) V. Balzani, A. Credi, F. M. Raymo, J. F. Stoddart, *Angew. Chem.* **2000**, *112*, 3484–3530; *Angew. Chem. Int. Ed.* **2000**, *39*, 3348–3391; b) C. A. Schalley, K. Beizai, F. Vogtle, *Acc. Chem. Res.* **2001**, *34*, 465–476; c) J.-P. Collin, C. Dietrich-Buchecker, P. Gaviña, M. C. Jimenez-Molero, J.-P. Sauvage, *Acc. Chem. Res.* **2001**, *34*, 477–487; d) T. R. Kelly, *Acc. Chem. Res.* **2001**, *34*, 514–522; e) G. S. Kottas, L. I. Clarke, D. Horinek, J. Michl, *Chem. Rev.* **2005**, *105*, 1281–1376; f) K. Kinbara, T. Aida, *Chem. Rev.* **2005**, *105*, 1377–1400; g) W. R. Browne, B. L. Feringa, *Nat. Nanotechnol.* **2006**, *1*, 25–35; h) B. L. Feringa, *J. Org. Chem.* **2007**, *72*, 6635–6652; i) E. R. Kay, D. A. Leigh, F. Zerbetto, *Angew. Chem.* **2007**, *119*, 72–196; *Angew. Chem. Int. Ed.* **2007**, *46*, 72–191; j) A. Coskun, M. Banaszak, R. D. Astumian, J. F. Stoddart, B. A. Grzybowski, *Chem. Soc. Rev.* **2012**, *41*, 19–30.

[2] a) M. Schliwa, *Molecular Motors*, Wiley-VCH, Weinheim, **2003**; b) D. S. Goodsell, *Bionanotechnology: Lessons from Nature*, Wiley, Hoboken, **2004**.

[3] For examples of unidirectional motion with artificial systems, see: a) T. R. Kelly, H. De Silva, R. A. Silva, *Nature* **1999**, *401*, 150–152; b) N. Koumura, R. W. J. Zijlstra, R. A. van Delden, N. Harada, B. L. Feringa, *Nature* **1999**, *401*, 152–155; c) D. A. Leigh, J. K. Y. Wong, F. Dehez, F. Zerbetto, *Nature* **2003**, *424*, 174–179; d) S. P. Fletcher, F. Dumur, M. M. Pollard, B. L. Feringa, *Science* **2005**, *310*, 80–82; e) T. Muraoka, K. Kinbara, T. Aida, *Nature* **2006**, *440*, 512–515; f) G. Haberhauer, *Angew. Chem.* **2008**, *120*, 3691–3694; *Angew. Chem. Int. Ed.* **2008**, *47*, 3635–3638; g) A. Martinez, L. Guy, J.-P. Dutasta, *J. Am. Chem. Soc.* **2010**, *132*, 16733–16734; h) N. Ruangsupapichat, M. M. Pollard, S. R. Harutyunyan, B. L. Feringa, *Nat. Chem.* **2011**, *3*, 53–60.

[4] Several synthetic helical molecules and polymers exhibit extension–contraction motion triggered by external stimuli, but these helical systems have rarely undergone a unidirectional twisting motion. For examples of their extension–contraction motions, see: a) O.-S. Jung, Y. J. Kim, Y.-A. Lee, J. K. Park, H. K. Chae, *J. Am. Chem. Soc.* **2000**, *122*, 9921–9925; b) E. Yashima, K. Maeda, O. Sato, *J. Am. Chem. Soc.* **2001**, *123*, 8159–8160; c) M. Barboiu, J. M. Lehn, *Proc. Natl. Acad. Sci. USA* **2002**, *99*, 5201–5206; d) M. Barboiu, G. Vaughan, N. Kyritsakas, J. M. Lehn, *Chem. Eur. J.* **2003**, *9*, 763–769; e) E. Berni, B. Kauffmann, C. Bao, J. Lefeuvre, D. M. Bassani, I. Huc, *Chem. Eur. J.* **2007**, *13*, 8463–8469; f) H.-J. Kim, E. Lee, H.-s. Park, M. Lee, *J. Am. Chem. Soc.* **2007**, *129*, 10994–10995; g) V. Percec, J. G. Rudick, M. Peterca, P. A. Heiney, *J. Am. Chem. Soc.* **2008**, *130*, 7503–7508; h) T. Hashimoto, T. Nishimura, J. M. Lim, D. Kim, H. Maeda, *Chem. Eur. J.* **2010**, *16*, 11653–11661; i) Y. Ferrand, Q. Gan, B. Kauffmann, H. Jiang, I. Huc, *Angew. Chem.* **2011**, *123*, 7714–7717; *Angew. Chem. Int. Ed.* **2011**, *50*, 7572–7575; j) M. Numata, D. Kinoshita, N. Hirose, T. Kozawa, H. Tamiaki, Y. Kikkawa, M. Kanesato, *Chem. Eur. J.* **2013**, *19*, 1592–1598; see also Ref. [5].

[5] a) K. Miwa, Y. Furusho, E. Yashima, *Nat. Chem.* **2010**, *2*, 444–449; b) K. Miwa, K. Shimizu, H. Min, Y. Furusho, E. Yashima, *Tetrahedron* **2012**, *68*, 4470–4478.

[6] For example, titin, which is a giant sarcomeric protein in cardiac and skeletal muscles, provides a springlike motion controlled by calcium-responsive conformational changes: a) H. Granzier, S. Labeit, *J. Physiol.* **2002**, *541*, 335–342; b) C. A. Opitz, M. Kulke, M. C. Leake, C. Neagoe, H. Hinssen, R. J. Hajjar, W. A. Linke, *Proc. Natl. Acad. Sci. USA* **2003**, *100*, 12688–12693; c) D. Labeit, K. Watanabe, C. Witt, H. Fujita, Y. Wu, S. Lahmers, T. Funck, S. Labeit, H. Granzier, *Proc. Natl. Acad. Sci. USA* **2003**, *100*, 13716–13721; d) M. M. LeWinter, Y. Wu, S. Labeit, H. Granzier, *Clin. Chim. Acta* **2007**, *375*, 1–9.

[7] H. Katagiri, T. Miyagawa, Y. Furusho, E. Yashima, *Angew. Chem.* **2006**, *118*, 1773–1776; *Angew. Chem. Int. Ed.* **2006**, *45*, 1741–1744.

[8] Y. Furusho, K. Miwa, R. Asai, E. Yashima, *Chem. Eur. J.* **2011**, *17*, 13954–13957.

[9] For examples of free-base bisporphyrins that sandwich aromatic guests in organic media, see: a) H. Iwamoto, M. Yamaguchi, S. Hiura, Y. Fukazawa, *Heterocycles* **2004**, *63*, 2005–2011; b) T. Haino, T. Fujii, Y. Fukazawa, *J. Org. Chem.* **2006**, *71*, 2572–2580; c) M. Tanaka, K. Ohkubo, C. P. Gros, R. Guilard, S. Fukuzumi, *J. Am. Chem. Soc.* **2006**, *128*, 14625–14633; d) T. Haino, T. Fujii, A. Watanabe, U. Takayanagi, *Proc. Natl. Acad. Sci. USA* **2009**, *106*, 10477–10481; e) T. Ema, N. Ura, K. Eguchi, Y. Ise, T. Sakai, *Chem. Commun.* **2011**, *47*, 6090–6092; f) T. Ema, N. Ura, K. Eguchi, T. Sakai, *Bull. Chem. Soc. Jpn.* **2012**, *85*, 101–109; g) T. Haino, A. Watanabe, T. Hirao, T. Ikeda, *Angew. Chem.* **2012**, *124*, 1502–1505; *Angew. Chem. Int. Ed.* **2012**, *51*, 1473–1476; h) A. Chaudhary, S. P. Rath, *Chem. Eur. J.* **2012**, *18*, 7404–7417; for a review, see: i) D. Margetic, *Curr. Org. Chem.* **2012**, *16*, 829–851.

[10] a) J. P. Collman, C. M. Elliott, T. R. Halbert, B. S. Tovrog, *Proc. Natl. Acad. Sci. USA* **1977**, *74*, 18–22; b) C. K. Chang, M.-S. Kuo, C.-B. Wang, *J. Heterocycl. Chem.* **1977**, *14*, 943–945; c) J. P. Collman, P. S. Wagenknecht, J. E. Hutchison, *Angew. Chem.* **1994**, *106*, 1620–1639; *Angew. Chem. Int. Ed. Engl.* **1994**, *33*, 1537–1554.

[11] Each type of porphyrin hydrogen atom in ligand **6a** showed one set of resonances in the ^{1}H NMR spectrum. In contrast, the helicate exhibited a pair of resonances in each case owing to the nonequivalent pyrrole hydrogen atoms; thus, the ^{1}H NMR spectrum indicated a twisted orientation of the face-to-face porphyrin units of the helicate.

[12] a) N. Harada, K. Nakanishi, *Circular Dichroic Spectroscopy: Exciton Coupling in Organic Stereochemistry*, University Science Books, Mill Valley, CA, **1983**; b) N. Berova, K. Nakanishi, R. W. Woody, *Circular Dichroism: Principles and Applications*, Wiley, New York, **2000**; c) N. Berova, L. D. Bari, G. Pescitelli, *Chem. Soc. Rev.* **2007**, *36*, 914–931; d) N. Berova, P. L. Polavarapu, K. Nakanishi, R. W. Woody, *Comprehensive Chiroptical Spectroscopy*, Wiley, Hoboken, **2012**.

[13] For CD studies on bisporphyrins, see: a) X. Huang, K. Nakanishi, N. Berova, *Chirality* **2000**, *12*, 237–255; b) V. V. Borovkov, G. A. Hembury, Y. Inoue, *Acc. Chem. Res.* **2004**, *37*, 449–459; c) G. A. Hembury, V. V. Borovkov, Y. Inoue, *Chem. Rev.* **2008**, *108*, 1–73; d) N. Berova, G. Pescitelli, A. G. Petrovic, G. Proni, *Chem. Commun.* **2009**, 5958–5980; e) I. C. Pintre, S. Pierrefixe, A. Hamilton, V. Valderrey, C. Bo, P. Ballester, *Inorg. Chem.* **2012**, *51*, 4620–4635.

[14] This association constant is significantly larger than those ($K_a \leq 10^6$) reported for bisporphyrin hosts and electron-deficient aromatic flat guests, including **G1** and **G2**, in organic media.[9]

[15] The present helicate has potential for use as a chiral shift reagent, since chiral recognition of the helicate enantiomers by various enantiomerically pure organic ammonium salts was possible, as supported by ^{1}H NMR spectra, which showed peaks due to the corresponding diastereomers (see Figure S19). Thus, the enantiomerically pure helicate should be capable of the chiral discrimination of the enantiomers of racemic ammonium salts on the basis of ^{1}H NMR spectroscopy.

